Dear Reviewer, #1

Thank you very much for your valuable comments. Our responses and the changes that we plan to make in the revised manuscript are explained below. We filled in reviewer comments in black, author replies in blue, the proposed changes to the revised manuscript in red.

Reviewer comment:

In this paper entitled "Characteristics of snowpack chemistry on the coastal region in the northwestern Greenland Ice Sheet facing the North Water", authors present an interesting observation of the effect that polynia North water (NOW) has on aerosol circulation and precipitation. the results are obtained from measurements of major ions, MSA and water isotopic analyses at 9 surface snow sampling sites, 2 snow-pit sites and 1 ice core. The text is well structured a detailed introduction, however the drafting in general should be improved as there are numerous repetitions and in some parts the reading is difficult to understand. In particular, the section 3.2 has to be improved. The conclusions have to be focused on the main goals obtained in this paper. It is very long and I suggest to summarize, avoiding to repeat the results and discussion.

Author reply:

To improve the overall logical flow and readability in section 3.2, we will add individual sub-sections for $\delta^{18}O$ and ion species. Figures of $\delta^{18}O$ and each ion concentration will be presented separately within their respective sub-sections.

We will summarize the conclusion section as follows and avoid some repetitions.

=====

4 Conclusion

We conducted glaciological observations from 9−11 April 2023 on the western side of Prudhoe Land in northwestern Greenland facing the NOW to elucidate the source conditions and transportation processes of water vapor and aerosols in this region. The dating of the snowpack at St. 9, which is located at the inland of the western side of Prudhoe Land, revealed that the layer at a depth of 4.20 m corresponded to 3.5 years. The average annual accumulation at St. 9 was 0.49 m w.eq. yr^{-1}.

The snowpacks on the western side of Prudhoe Land contained aerosols from distant sources, such as remote dust and anthropogenic aerosols, in early spring‑summer layers. On the other hand, they also contained aerosols from local sources such as ocean biological activity and frost flowers in the NOW and local dust around the coast of northwestern Greenland during other seasons, unlike the inland of the Greenland Ice Sheet. Moreover, we noted that the snowpacks were able to trace the poleward heat and moisture transport event along Baffin Bay during winter.

Arctic climate warming caused decreases in the sea ice thickness and concentration over the last few decades in the NOW and could influence clouds and precipitation following changes in sea ice and biological activities in the NOW. We found for the first time that the environmental changes in the NOW can be elucidated by the snowpack and ice core on the western side of the Prudhoe Land. We suggest that the chemical substances in the deeper ice core from this region could help explain the multidecadal variations in the sea ice, biological activities, and related water and aerosol circulation around the NOW and could develop to understand the accurate future projections of environmental change in this region.

=====

Reviewer comment:

On lines105-106: "The snow sampling intervals at St. 3 were 0.02 m from 0.00 to 0.20 m and 0.03 m from 0.20 to 1.01 m, and the snow sampling intervals at St. 9 were 0.02 m from 0.00 to 0.20 m and 0.03 m from 0.30 to 1.08 m." Why was the sampling interval changed?

Author reply:

If we could sample the entire snowpack at short intervals, we would have been able to discuss the temporal variations in chemical components with short time intervals. However, we changed sampling interval partway through the snowpack, because we had limitation on the number of snow samples that could be transported by dog sledges.

Reviewer comment:

Lines 104, 108, 110. The authors told of precleaned materials and tools, but the cleaning procedure is not described.

Author reply:

We will add the cleaning procedure to the method section as follows.

=====

We removed the oil contamination on the precleaned materials and tools using ethanol, and performed then ultrasonic cleaning in ultrapure water.

=====

Reviewer comment:

On line 107: Why was the ice core only sampled at one site? could be used for comparison at least with st3.

Author reply:

We prioritized sampling as much as possible at St. 9 because of the limitation on the number of snow samples that could be transported by dog sledges.

Reviewer comment:

Line 115: "methane sulfonate− (hereafter referred to as MSA)" already defined in the introduction

Author reply:

The definition of MSA will be moved to the Introduction.

Reviewer comment:

Lines 116-118. Please add several details about the analytical methods or some references. In particular, the authors declared only the columns used for cations and anions without any specific important details such as dimensions. Other important details are flows, injection volumes, instruments used, suppressors, detectors. No specific details about the quantification methods are reported. I suppose that you used external calibration curves, but which are the linear ranges, and which are the RCM used for quantification. In summary, please improve the method and quality control section about the ionic analysis.

Author reply:

We will add details about the analytical method of the ion chromatography in the method section as follows.

=====

For the cations, separation was carried out with a Dionex CG-12 (4 × 50 mm) guard column, followed by a Dionex CS12-A (4 × 250 mm) separation column. Injection volume of samples was 500 µL. MSA (20 mM) was used as eluent, and flow-rate was kept 1.0 mL min-1. Dionex CDRS600 dynamically regenerated suppressor was used for conductivity suppression before conductivity cell. For the anions, separation was obtained with a Dionex AG-18 (4 × 50 mm) guard column and Dionex AS-18 (4 × 250 mm) separation column. Injection volume of samples was 1000 µL. KOH (23 mM) was used as eluent, and flow-rate was kept 1.0 mL min-1. Dionex ADRS 600 dynamically regenerated suppressor was used for conductivity suppression before conductivity cell. 5-point calibration curves were used for quantitative determination of each ion. The calibration curves were constructed using standard solution (Fujifilm Waco) adjusted to 20, 50, 100, and 200 ppb with ultra-pure water. If the ion concentration of samples were outside the calibration range (> 200 ppb), it was remeasured using 500, 1000, 2000~3000, and 6000 ppb standard for the anions and 500, 1000, 2000, and 4000 ppb standard for the cations. Blanks were always evaluated before the calibration procedure.

=====

Reviewer comment:

Lines 117-119: Has the ion chromatography method used been validated in previous works? If yes, indicate them, if not, insert a section on validation.

Author reply:

The ion chromatography method had been validated by the previous work (Kurosaki et al., 2020; Kurosaki et al., 2022). We will add this description to the method section as follows.

=====

The ion chromatography method in this study had been evaluated by our previous study (Kurosaki et al., 2020; Kurosaki et al., 2022).

=====

Reviewer comment:

Lines 119-120: “The samples exhibiting large peak were measured multiple times, to confirm that any large peak in ion concentration was not caused by analytical errors.” What is meant?

Author reply:

The large peaks of Na^+ and Cl^- were outside the calibration range up to 200 ppb. These samples were remeasured using 500, 1000, 2000~3000, and 6000 ppb standard for the anions and 500, 1000, 2000, and 4000 ppb standard for the cations.

We will add this text to the method section as follows.

=====

The 5-point calibration curves were constructed using standard solution (Fujifilm Waco) adjusted to 20, 50, 100, and 200 ppb with ultra-pure water. If the ion concentration of samples were outside the calibration range (> 200 ppb), it was remeasured using 500, 1000, 2000~3000, and 6000 ppb standard for the anions and 500, 1000, 2000, and 4000 ppb standard for the cations. Blanks were always evaluated before the calibration procedure.

=====

Reviewer comment:

Lines 156-165 Text is not clear

Author reply:

We have revised the text you kindly pointed out as follows.

=====

We determined the seasonality of the snowpack from 0.00 to 1.15 m as shown below. The date of snow layer from 0.00–0.04 m was close to the observation date (April 2023). We determined that snowpack in 0.04–0.72 m corresponded to the autumn to winter period from 2022–2023 from the negative $\delta^{18}O$ peak, positive d-excess peak and low MSA values (Fig. 2). The snowpack from 0.72 m–1.15 m corresponded to spring to summer in 2022 from existence of ice layer, high $\delta^{18}O$ value and high MSA values (Fig. 2 and Fig. S2). Snowpack below 0.96 m corresponded to previous summer and before it because the amplitude of seasonal variation of $\delta^{18}O$ and d-excess below 0.96 m were smaller than those in the shallower layers from 0.00–0.96 m because of summer melting (Fig. 2a and b). The MSA concentration showed obvious seasonal variations, and the $\delta^{18}O$ values exhibited slight seasonal variations below 0.96 m (Fig. 2a and c), although the values of the water stable isotopes were smoothed by summer melting and some chemical species showed high peaks in the ice layers owing to relocation processes by meltwater refrozen.

=====

Reviewer comment:

Section 3.2. Following stratigraphic analysis and evaluation of snowpack density, it may be more informative to express data in terms of fluxes rather than concentrations, so in the subsequent data analysis one could avoid distinguishing peaks attributed to atmospheric deposition from those of melting and refreezing

Author reply:

As you have pointed out, the deposition flux is sometimes more suitable when discussing the deposition amount of atmospheric aerosols for quantitatively. However, we cannot discuss the deposition flux because we did not collect the snow density with high resolution along the snow depth. Therefore, we qualitatively discussed the seasonal characteristics of ion species based on their concentration.

Reviewer comment:

Lines 188–190: Introducing all figures at the beginning of the section may lead to confusion. Since the discussion begins with Fig. 5, it would be more effective to present the figures sequentially, in alignment with the narrative.

Author reply:

In accordance with your comment, we will revise the order of figures. We will present the $\delta^{18}O$ and each ion concentration within the relevant sub-sections of section 3.2, displaying the figures sequentially.

Reviewer comment:

Line 194: "We applied the concentration unit as μeq L−" Information that is already made explicit in the following graphs

Author reply:

This sentence notes that "μ eq L^{-1}" was used as the unit of ion concentration in equation (1). The editor requested that the concentration unit should state clearly for the equation (1).

Reviewer comment:

Line 201: "We suggest that the spatial variation in the $\delta^{18}O$ results from water vapor transport from the southern coast to the northern inland area by southerly winds." Might it be useful to indicate figure 9 by referring to the direction of the prevailing winds?

Author reply:

Thank you for your comment. We suggested that the south-to-north gradient of the $\delta^{18}O$ results from water vapor from the southern coast to northern inland area by the southerly winds. We have performed the backward trajectory analysis and analyzed the probability map of air mass transportation to make this assumption more reliable (Fig. 1 in this file). The 7-days backward trajectory of air mass arriving at St. 9 showed that the majority of air mass was transported from the south of St. 9, situated on northern Baffin Bay and eastern NOW.

We will add the method of backward trajectory in section 2.3 as follows.

=====

2.3 Backward trajectory

To investigate the source region and transport pathway of water vapor and aerosols contained in ice core at the St. 9 site, we analysed air mass position along the backward trajectory from the St. 9 site during the past 7 days using the National Oceanographic and Atmospheric Administration (NOAA) Hybrid Single-Particle Lagrangian Integrated Trajectory (HYSPLIT) model (Stein et al., 2015) and National Centers for Environmental Prediction (NCEP) reanalysis data. The initial positions of air mass were set at 50, 500, 1000, 1500 m above ground level over the St. 9 site. The initial date and time were every 6 h from 2019 to 2023. We calculated the probability of the existence of an air mass with a 1° resolution. Considering the water vapor and aerosols supply from the ocean and land surface, we excluded air mass over 1000 m above ground level. The existence probability was weighted by the daily amount of precipitation when the air mass arrived at the St. 9 site. The daily amount of precipitation was extracted from the ERA5 reanalysis dataset (Hersbach et al., 2020).

=====

We will revise the early part of result and discussion of the $\delta^{18}O$ (section 3.2.1) as follows. Figure 1 in this file will be added to the supplementary material.

=====

3.2.1 $\delta^{18}O$

The spatial variations in $\delta^{18}O$ in the surface snow showed maximum and minimum values at St. 3 (−19.12 ‰) and St. 9 (−37.21 ‰), respectively (Fig. S4a). The average $\delta^{18}O$ value from 0.00 to 1.01 m at St. 3 was greater than that at St. 9 (St. 3: −22.03 ‰; St. 9: −29.12 ‰) (Table 1). The $\delta^{18}O$ values in surface snow and the snowpack decreased from the seacoast toward the inland site. The past 7 days backward trajectory arriving at the St. 9 also exhibited that majority of air mass was transported from the south of the St. 9, situated on the northern Baffin Bay and eastern NOW (Fig. S5). We suggest that the south-to-north gradient of $\delta^{18}O$ results from water vapor, which originates from northern Baffin Bay and eastern NOW, transport from the southern coast to the northern inland area by southerly winds.

=====

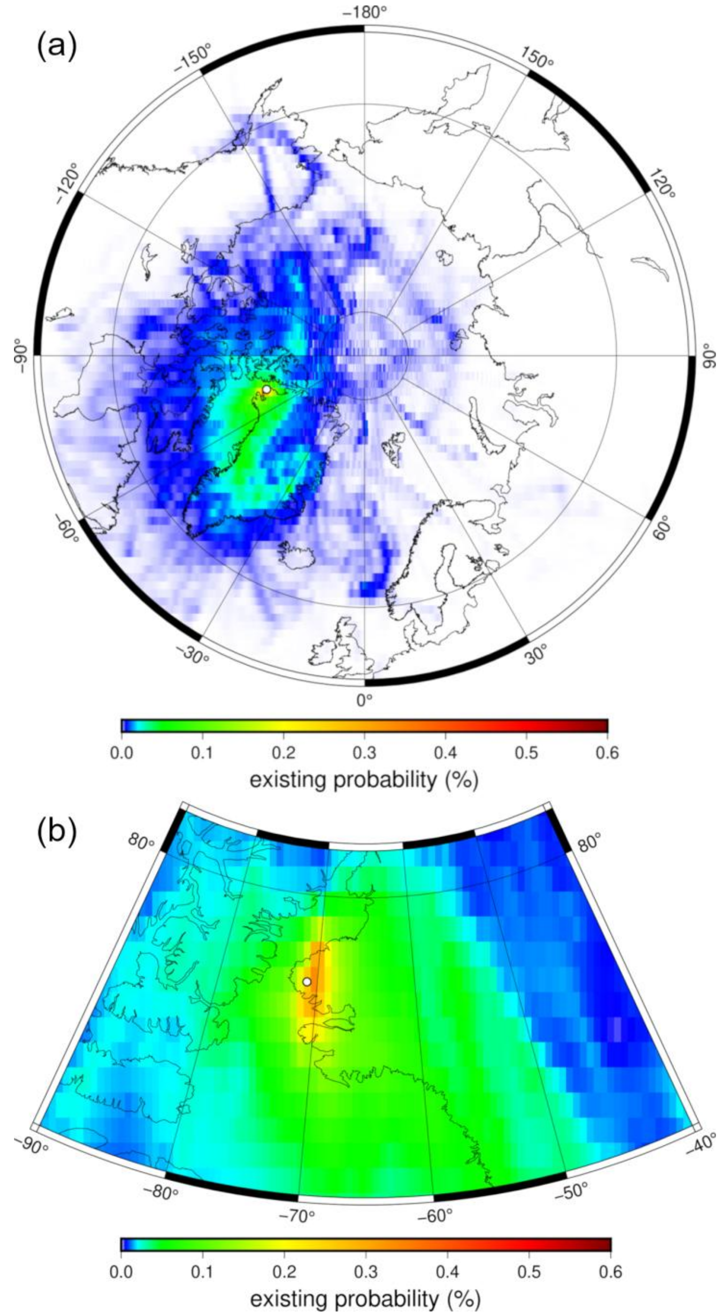

Figure 1 (in this file): Existence probability of an air mass occurring during the past during 7 days reaching the St. 9 in whole of year from 2019–2023. (a) and (b) display Arctic area (> 60°N) and around northwestern Greenland, respectively. Black circles show the position of the St. 9.

Reviewer comment:

Line 210. Please add "(figure 6)" to help readers or start the sentence introducing the Figure 6 and its meaning.

Author reply:

The explanation of related figure will be added at the beginning of the paragraph about the vertical profile of $\delta^{18}O$ at St. 3 and St. 9 as follows.

=====

Fig. 3 shows the vertical profile of $\delta^{18}O$ in the snowpack at St. 3 and St. 9, and the difference in $\delta^{18}O$ between St. 9 and St. 3. The vertical profile of $\delta^{18}O$ in the snowpacks at St. 9 was similar to that at St. 3.

=====

Reviewer comment:

Figure 6: I suggest using the season and year instead of Roman numerals, as this would facilitate interpretation. This recommendation may also apply to the other figures. It is somewhat difficult to follow the discussion, as it requires frequently switching between different figures.

Author reply:

To improve the overall logical flow and readability in section 3.2, we will add individual sub-sections for $\delta^{18}O$ and ion species. Figures of $\delta^{18}O$ and each ion concentration will be presented separately within their respective sub-sections. The seasonal divisions in each figure will be revised from Roman numerals to explicit labels indicating the season and year (ex. Fig. 2 in this file).

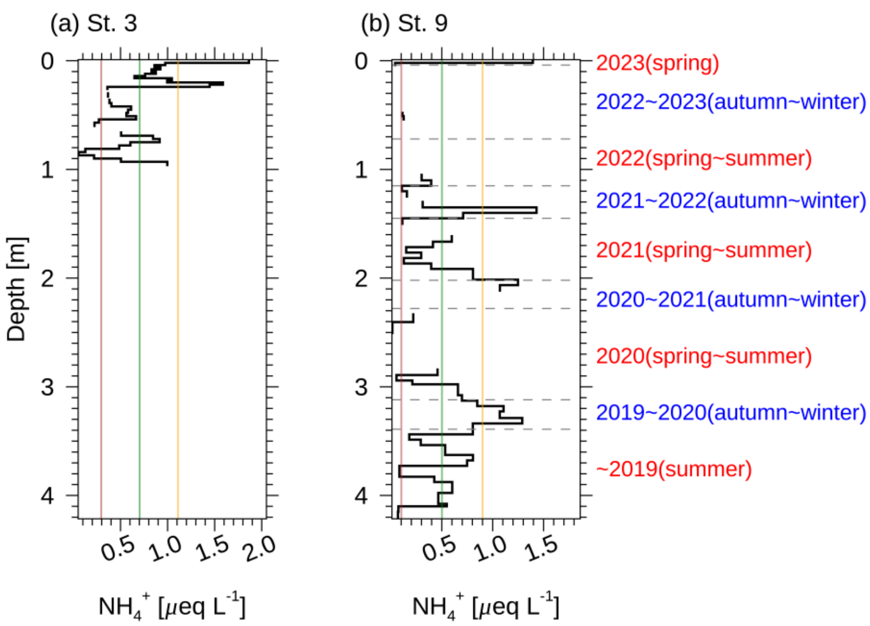

Figure 2 (in this file): Vertical profile of NH_4^+ at (a) St. 3 and (b) St. 9. Green lines denote mean NH_4^+ across all observation depths. Orange and brown lines denote the mean NH_4^+ plus and minus one standard deviation across all observation depths, respectively. The LOD of NH_4^+ was < 0.0055 μeq L^{-1}.

Reviewer comment:

Figure 6c, it is not clear why the authors used the difference between St3 and St.9, instead of a ratio.

Author reply:

To discuss the seasonal variation of the surface air temperature difference between St. 3 and St. 9, we calculated the difference of $\delta^{18}O$ values at the two stations.

We propose that the difference between St. 3 and St. 9 can be discussed for the following reasons.
The depths of the negative and positive peaks of $\delta^{18}O$ at St. 9 agreed well with those at St. 3 (Fig. 3 in this file), and the vertical profile of $\delta^{18}O$ between 0.00 and 1.01 m at St. 9 correlated significantly with that at St. 3 ($r = 0.69$, $p < 0.01$). The snowpack corresponding to autumn−winter from 2022−2023 at St. 3 and St. 9 at the same snow depth were most likely accumulated with precipitation attributed to the same snowfall events, and $\delta^{18}O$ in the snowpack had not been changed by the post depositional processes, which is water molecule diffusion, wind blowing, and sublimation. Therefore, we propose that the vertical profile of $\delta^{18}O$ between 0.00 and 1.01 m at St. 9 can be reasonably compared with the profile at St. 3 based on their differences.
We have already described the above discussion in our manuscript.

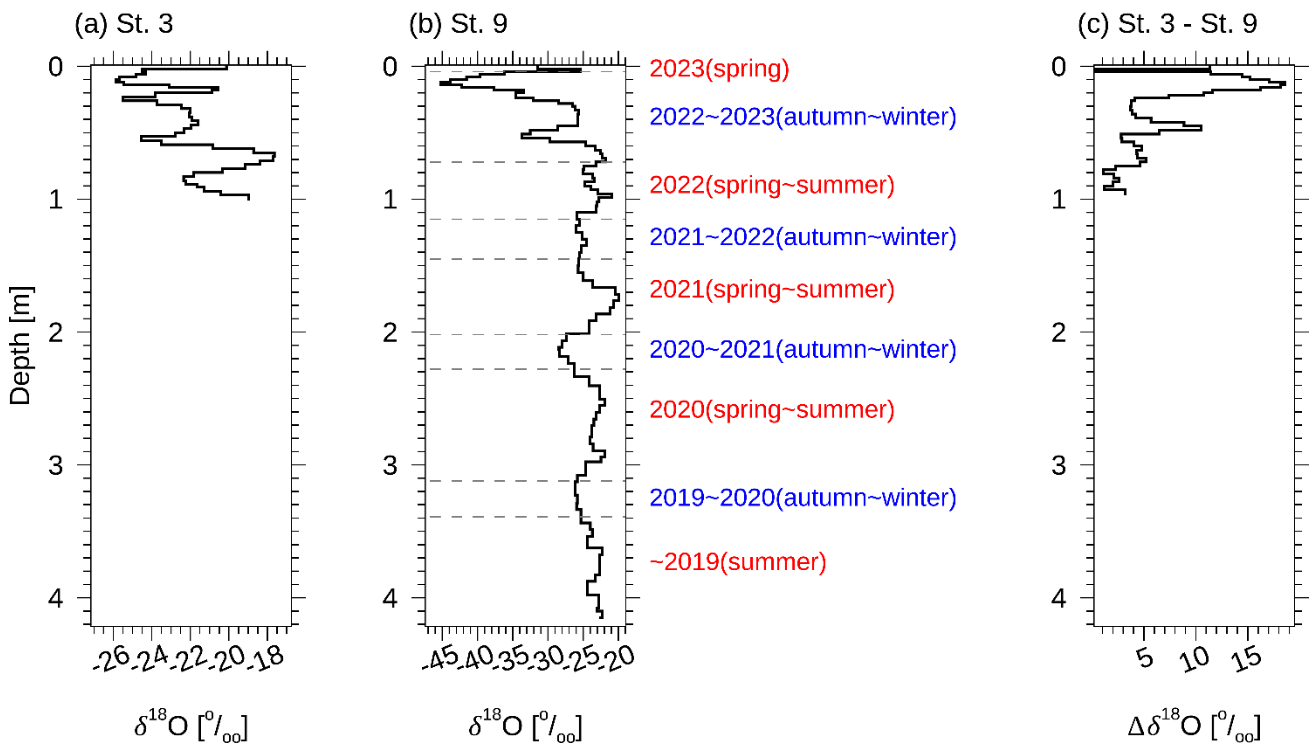

Figure 3 (in this file): Vertical profile of $\delta^{18}O$. (a) and (b) show $\delta^{18}O$ values at St. 3 and St.9, respectively. (c) shows difference between St.3 and St.9 in terms of $\delta^{18}O$. i–vii denote seasons from 2019 to 2023. i, iii, v, and vii denote from autumn to winter period from 2022–2023, 2021–2022, 2020–2021, and 2019–2020, respectively. ii, iv, and vi denote from spring to summer in 2022, 2021, and 2020, respectively.

Reviewer comment:

Line 217-218: "We suggest that the altitude gradient of the surface air temperature in winter was greater than that in summer in the western region of Prudhoe Land." could this statement also be confirmed using atmospheric models for specific sites?

Author reply:

We estimated the difference in surface air temperature between St. 9 and St. 3 using ERA5-Land reanalysis dataset (Fig. 4 and Fig. 5 in this file). The temperature difference between St. 9 and St. 3 was greatest in summer. The mean temperature differences in autumn and winter were more negative than that in summer. This result supports our suggestion, based on water stable isotope, that the altitude gradient of surface air temperature in the western side of Prudhoe Land was steeper in winter than in summer.

We will add this description in section 3.2.1 as follows. Figure 4 and 5 in this file will be added to the supplementary material.

=====

We estimated the difference in surface air temperature between St. 9 and St. 3 using ERA5-Land reanalysis dataset (Fig. S5 and Fig. S6). The temperature difference between St. 9 and St. 3 was greatest in summer. The mean temperature differences in autumn and winter were more negative than that in summer. This result supports our suggestion, based on water stable isotope, that the altitude gradient of surface air temperature in the western side of Prudhoe Land was steeper in winter than in summer.

=====

We will add the explanation of ERA5-Land in the method section as follows.

=====

Additionally, we used 2 m air temperature in the western side of the Prudhoe Land from ERA5-Land reanalysis dataset supplied by the ECMWF (Muñoz-Sabater et al., 2021)

=====

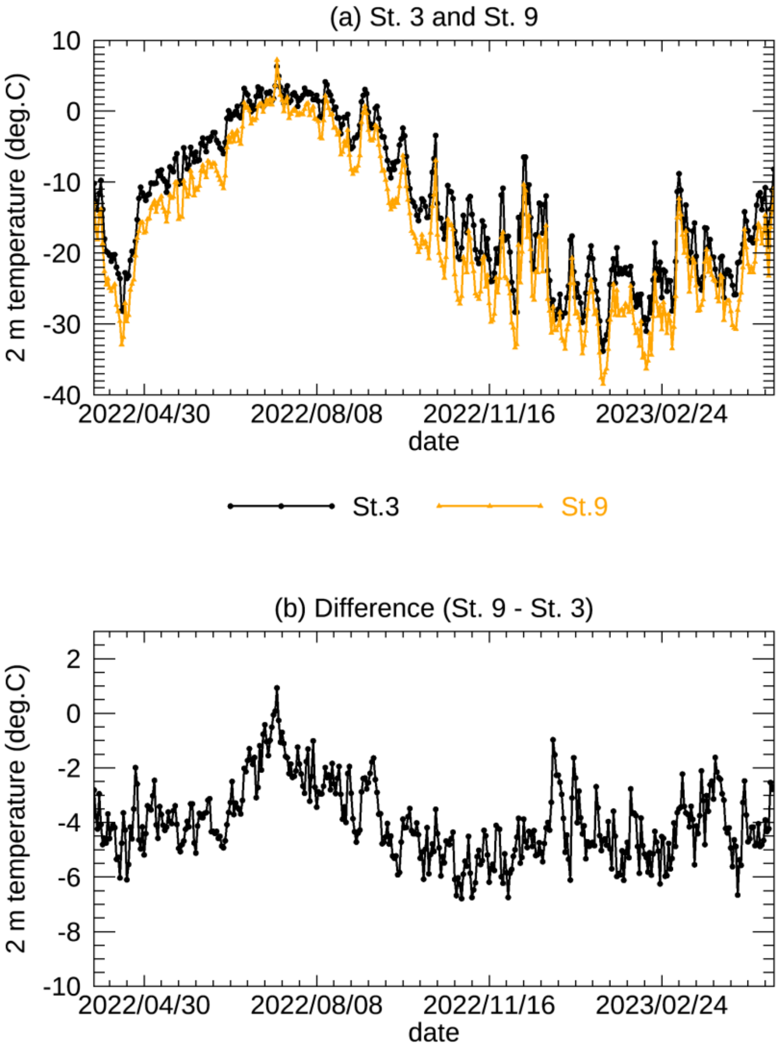

Figure 4 (in this file): Diurnal variations in (a) 2 m air temperature at St. 3 and St. 9, and (b) 2 m air temperature difference between St. 9 and St. 3.

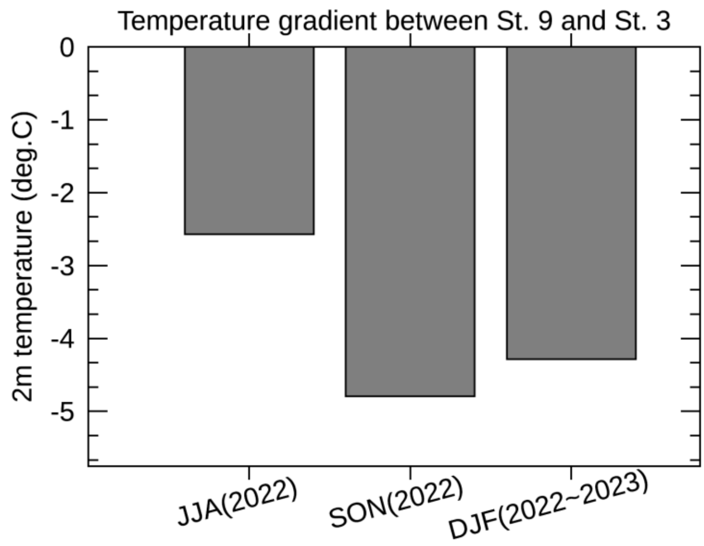

Figure 5 (in this file): Seasonal variations in the difference of 2 m air temperature between St. 9 and St. 3.

Reviewer comment:

Lines 306-309: there are many repetitions of "the concentration of MSA". Same in the conclusions with "The snowpack on the western side of Prudhoe Land".

Author reply:

Thank you for your kind comment. We will revise the text that you have pointed out as follows.

=====

3.2.7 MSA

MSA is an oxidation product of DMS, which originates from ocean phytoplankton (Charlson et al., 1987; Jaffrezo et al., 1994). The concentration of MSA in surface snow reached a maximum value at St. 6 (Fig. S4j). At St. 3, an exceptionally high MSA was observed at a depth of 1.01 m, corresponding to the summer of 2022 (Fig. 9a). The snowpack at St. 9 exhibited multiple distinct MSA peaks at depths of 0.83, 1.07, 2.68, 2.91, and 3.57 m (Fig. 9b).

4 Conclusion

We conducted glaciological observations from 9−11 April 2023 on the western side of Prudhoe Land in northwestern Greenland facing the NOW to elucidate the source conditions and transportation processes of water vapor and aerosols in this region. The dating of the snowpack at St. 9, which is located at the inland of the western side of Prudhoe Land, revealed that the layer at a depth of 4.20 m corresponded to 3.5 years. The average annual accumulation at St. 9 was 0.49 m w.eq. yr^{-1}.

The snowpacks on the western side of Prudhoe Land contained aerosols from distant sources, such as remote dust and anthropogenic aerosols, in early spring–summer layers. On the other hand, they also contained aerosols from local sources such as ocean biological activity and frost flowers in the NOW and local dust around the coast of northwestern Greenland during other seasons, unlike the inland of the Greenland Ice Sheet. Moreover, we noted that the snowpacks were able to trace the poleward heat and moisture transport event along Baffin Bay during winter.

Arctic climate warming caused decreases in the sea ice thickness and concentration over the last few decades in the NOW and could influence clouds and precipitation following changes in sea ice and biological activities in the NOW. We found for the first time that the environmental changes in the NOW can be elucidated by the snowpack and ice core on the western side of the Prudhoe Land. We suggest that the chemical substances in the deeper ice core from this region could help explain the multidecadal variations in the sea ice, biological activities, and related water and aerosol circulation around the NOW and could develop to understand the accurate future projections of environmental change in this region.

=====

Reviewer comment:

General comment on the conclusions: from figure 1 sampling sites 1 to 5 (or 6) are in a valley. has this aspect been taken into consideration? could it have an impact on the final considerations?

Author reply:

I appreciate your valuable comment.

Because the topography in the western side of Prudhoe Land is smooth (Fig. 1 in this file) and the glacier is broad and relatively low gradient, we think that the enhancement of vertical convection and downslope wind caused by the valley topography are insignificant on the large-scale water vapor and aerosol circulation around the western side of the Prudhoe Land.

Other comments:

Reviewer comment:

In figure 1b it might be useful to include a dimensional scale to give an idea of the distances.

Similarly, in figure 2, in addition to the distance expressed in latitude, could a conversion to km be useful?

Author reply:

Thank you for your ideas. We have added the scale of distance and north arrow (Fig. 6 in this file), and the distance from St. 1 to each sampling station (Fig. 7 in this file).

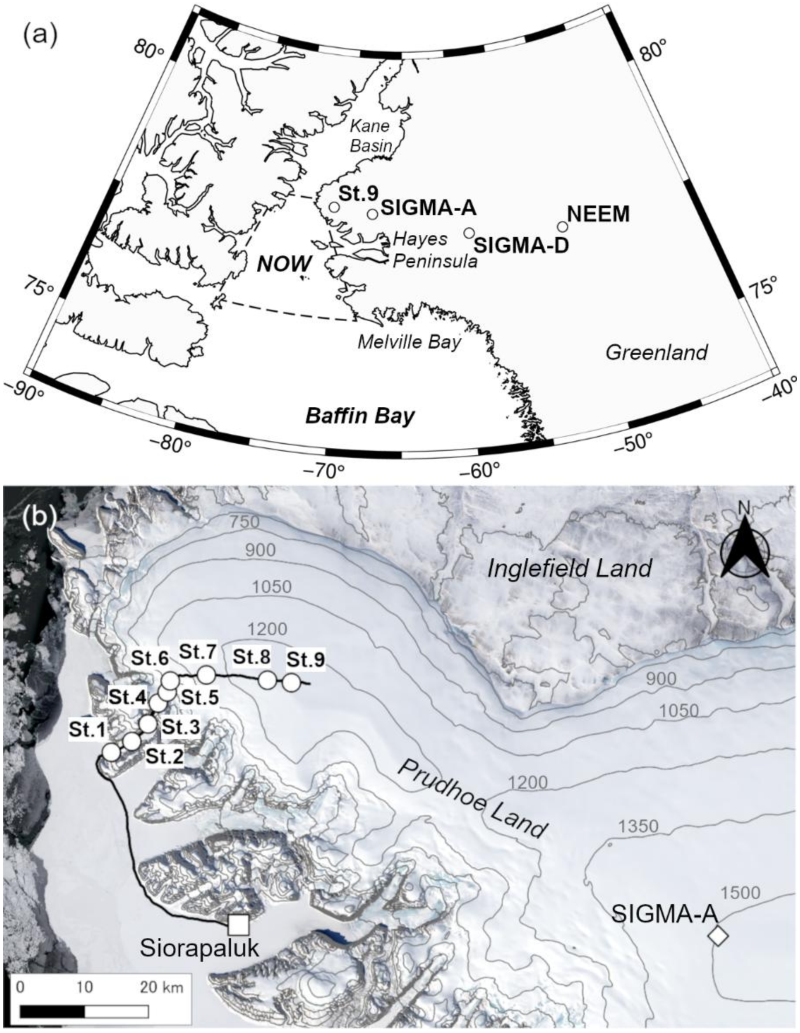

Figure 6 (in this file): Maps of the sampling sites. (a) shows location of the snowpit and ice core sampling sites in this study (St. 9) and previous studies (SIGMA-A, SIGMA-D, and NEEM) in the northwestern Greenland Ice Sheet. The dashed polygon in (a) denotes the approximate location of the NOW. Hayes peninsula in the northwestern Greenland is located between Kane Basin in the north and Melville Bay in the south. (b) shows Landsat-8 image around St. 9 and SIGMA-A of Prudhoe Land, which is located on the northern part of Hayes peninsula, on 13 April 2023. The black circles in (b) denote the sampling sites from St. 1 to St. 9, and the black line denotes dog sledge route. The gray contours in (b) are drawn from the Greenland Mapping Project 2 (GIMP-2) Digital Elevation Model version 2.

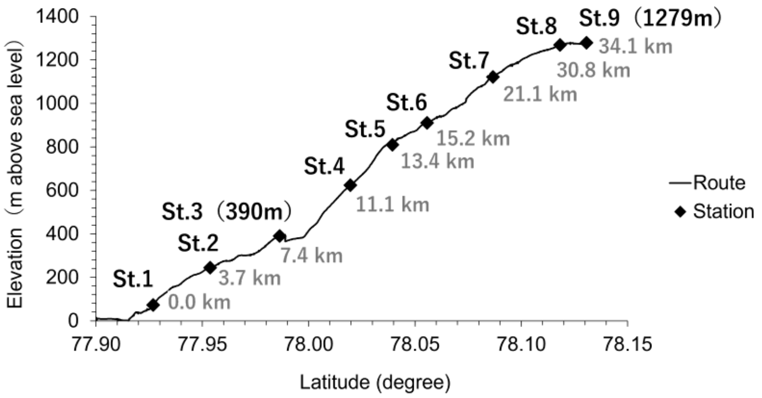

Figure. 7 (in this file): Elevation above sea level of each station. Gray values denote the distance from St. 1 to each station.

Reviewer comment:

In figure 5, in addition to changing colours between total and nss values, it would also be useful to change the symbols

Author reply:

Symbols will be removed from the figure corresponding to the vertical profile of $\delta^{18}O$ and ion species because we will plot the step-width graph. The example of figure corresponding to the vertical profile of $\delta^{18}O$ and ion species was shown in Fig. 2 and Fig. 3 in this file.

Reference:

Charlson, R. J., Lovelock, J. E., Andreae, M. O., and Warren, S. G.: Oceanic phytoplankton, atmospheric sulphur, cloud albedo and climate, Nature, 326, 655–661, https://doi.org/10.1038/326655a0, 1987.

Jaffrezo, J.-L., Davidson, C. I., Legrand, M., and Dibb, J. E.: Sulfate and MSA in the air and snow on the Greenland Ice Sheet, J. Geophys. Res. Atom., 99, 1241–1253, https://doi.org/10.1029/93JD02913, 1994.

Hersbach, H., Bell, B., Berrisford, P., Hirahara, S., Horányi, A., Muñoz-Sabater, J., Nicolas, J., Peubey, C., Radu, R., Schepers, D., Simmons, A., Soci, C., Abdalla, S., Abellan, X., Balsamo, G., Bechtold, P., Biavati, G., Bidlot, J., Bonavita, M., De Chiara, G., Dahlgren, P., Dee, D., Diamantakis, M., Dragani, R., Flemming, J., Forbes, R., Fuentes, M., Geer, A., Haimberger, L., Healy, S., Hogan, R. J., Hólm, E., Janisková, M., Keeley, S., Laloyaux, P., Lopez, P., Lupu, C., Radnoti, G., De Rosnay, P., Rozum, I., Vamborg, F., Villaume, S., and Thépaut, J.: The ERA5 global reanalysis, Quart J Royal Meteoro Soc, 146, 1999–2049, https://doi.org/10.1002/qj.3803, 2020.

Kurosaki, Y., Matoba, S., Iizuka, Y., Niwano, M., Tanikawa, T., Ando, T., Hori, A., Miyamoto, A., Fujita, S., and Aoki, T.: Reconstruction of Sea Ice Concentration in Northern Baffin Bay Using Deuterium Excess in a Coastal Ice Core From the Northwestern Greenland Ice Sheet, JGR Atmospheres, 125, e2019JD031668, https://doi.org/10.1029/2019JD031668, 2020.

Kurosaki, Y., Matoba, S., Iizuka, Y., Fujita, K., and Shimada, R.: Increased oceanic dimethyl sulfide emissions in areas of sea ice retreat inferred from a Greenland ice core, Commun Earth Environ, 3, 327, https://doi.org/10.1038/s43247-022-00661-w, 2022.

Muñoz-Sabater, J., Dutra, E., Agustí-Panareda, A., Albergel, C., Arduini, G., Balsamo, G., Boussetta, S., Choulga, M., Harrigan, S., Hersbach, H., Martens, B., Miralles, D. G., Piles, M., Rodríguez-Fernández, N. J., Zsoter, E., Buontempo, C., and Thépaut, J.-N.: ERA5-Land: a state-of-the-art global reanalysis dataset for land applications, Earth Syst. Sci. Data, 13, 4349–4383, https://doi.org/10.5194/essd-13-4349-2021, 2021.

Stein, A. F., Draxler, R. R., Rolph, G. D., Stunder, B. J. B., Cohen, M. D., and Ngan, F.: NOAA's HYSPLIT Atmospheric Transport and Dispersion Modeling System, Bulletin of the American Meteorological Society, 96, 2059–2077, https://doi.org/10.1175/BAMS-D-14-00110.1, 2015.